International Journal of Engineering

Journal Homepage: www.ije.ir

Effect of Different Turbine-generator Shaft Models on the Sub-synchronous Resonance Phenomenon in the Double Cage Induction Generator Based Wind Farm

M. K. Salehi, R. Zeinali Davarani*

Faculty of Electrical and Computer Engineering, Graduate University of Advanced Technology, Kerman, Iran

PAPER INFO

Paper history:
Received 07 February 2016
Received in revised form 14 July 2016
Accepted 14 July 2016

Keywords:
Double Cage Induction Generator
Turbine-Generator Shaft Model
Wind Farm
Torsional Modes
Sub-Synchronous Resonance

ABSTRACT

This paper focuses on the turbine-generator shaft models of double-cage Induction Generator (IG) based wind farm and its impact on the sub-synchronous resonance phenomenon. For this purpose, six different shaft models as 6-mass, 4-mass, 3-mass I, 3-mass II, 2-mass and 1-mass models are considered for double-cage IG wind-turbine. By using the linear modal analysis method, the effects of the different multi mass model of double-cage IG wind-turbine on the SSR phenomenon are studied. The results obtained by eigenvalue analysis show that the model of double-cage IG wind-turbine has an important effect on the detecting of Subsynchronous Resonance (SSR) phenomenon. The analytical results are validated by detailed electromagnetic transient simulation using PSCAD/EMTDC software.

***doi**: 10.5829/idosi.ije.2016.29.08b.10*

NOMENCLATURE

s	the induction generator slip	H_H	hub inertia
V_{ds} & V_{qs}	d-q axis voltage of the double-cage IG stator	H_{GB}	gearbox inertia
I_{ds} & I_{qs}	d-q axis current of the double-cage IG stator	H_G	generator inertia
I_{dr1} & I_{qr1}	d-q axis current of first rotor cage	V_{cd} & V_{cq}	d-q axis voltage across series capacitor
I_{dr2} & I_{qr2}	d-q axis current of second rotor cage	V_{bd} & V_{bq}	d-q axis voltage at infinite bus
R_s & $X_{s\sigma}$	resistance and unsaturated leakage reactance of stator winding, respectively	X_{Cg}	reactance of shunt capacitor
R_{r1} & $X_{r\sigma 1}$	resistance and unsaturated leakage reactance of first rotor cage, respectively	X_C	reactance of series capacitor
R_{r2} & $X_{r\sigma 2}$	resistance and unsaturated leakage reactance of second rotor cage, respectively	R	transmission line resistance
X_m	unsaturated magnetizing reactance	X_L	transmission line reactance
X_{rm}	unsaturated mutual leakage reactance between two rotor cages	X_t	reactance of transformer
T_G	generator electromagnetic torque	X_b	source reactance of infinite bus
H_{B1}, H_{B2} & H_{B3}	blade inertias	K	series compensation level (%)

1. INTRODUCTION

Installation of wind power plants is rapidly increasing due to their environmental benefits and the limitation of fossil-fuel resources [1]. As the integration of wind farms and electrical networks increases, the stability of power systems will gradually be affected by the characteristics of wind-turbines. Therefore, it is necessary to utilize the appropriate wind-turbine models to study the behavior of wind farms at different phenomena of the power system. Most wind farms across the world use doubly fed induction generators [2]. However, there are a large number of wind farms operating or under construction, which utilize self-excited induction generator based wind-turbines [3]. Between self-excited induction generators, the double-cage Induction Generator (IG) is preferred due to its

*Corresponding Author's Email: *r.zeinali@kgut.ac.ir* (R. Zeinali Davarani)

Please cite this article as: M. K. Salehi and R. Zeinali Davarani, Effect of Different Turbine-generator Shaft Models on the Sub-synchronous Resonance Phenomenon in the Double Cage Induction Generator Based Wind Farm, International Journal of Engineering (IJE), TRANSACTIONS B: Applications Vol. 29, No. 8, (August 2016) 1103-1111

high efficiency, mechanical simplicity, and low maintenance requirements [4].

Transmission capacity of existing lines may need to be enhanced to accommodate the large amounts of power from wind plants. Application of series capacitors in transmission lines is a well-known technology to increase the power transfer capability in a power system [5]. However, series capacitors may cause Sub-synchronous Resonance (SSR). There are two important aspects of the SSR: (i) self-excitation due to induction generator effect, (ii) torsional interaction. In the self-excitation phenomenon because of series compensation, the damping of sub-synchronous mode becomes negative and leads to instability of the power system. In the torsional interaction phenomenon, the series compensation can lead to turbine–generator shaft failure. Torsional interaction leads to decreasing of torsional modes damping and in the worst condition, it may lead to instability of torsional modes [6, 7].

In the literature, by time domain approach, various models of the wind-turbine are used to study different phenomena in power systems [8-14]. However, to analyze the SSR in wind farms normally a two mass model is considered to represent the dynamics of the wind turbine-generator shaft [15-24]. In this paper a comprehensive analysis of SSR potential in a double-cage IG based wind farm connected to series compensated line is presented. For this purpose, an in-depth mathematical model of the double-cage IG connected to series capacitor is developed along with a detailed model of the wind-turbine. By using the linear modal method, eigenvalue analysis is carried out, which is validated with electromagnetic transient simulation studies using PSCAD/EMTDC. Fast Fourier Transform (FFT) method is used to analyze the frequency spectrum of the signals obtained from PSCAD/EMTDC simulations and verify the eigenvalue analysis results [25].

The remainder of this paper is organized as follows. Section 2 describes the modeling of various subsystems including double-cage IG, turbine-generator shaft, ac transmission line, and their overall interconnection. Section 3 presents a detailed eigenvalue analysis of the system under different operating conditions. Validation of the eigenvalue results through time-domain simulation is also presented in section 4. Finally, section 5 concludes the paper.

2. SYSTEM DESCRIPTION

The studied system shown in Figure 1 consists of a wind farm supplying bulk power to an infinite bus over a long-distance series-compensated transmission line.

2. 1. Double Cage Induction Generator Model

The wind farm in the studied system is composed of many wind turbines based on the double-cage IGs. The positive sequence equivalent circuit of a double-cage IG is shown in Figure 2.

Differential equations of double-cage IG in the d-q frame can be expressed as

$$\frac{1}{\omega_s}\frac{d}{dt}\lambda_{ds} = -R_s I_{ds} + \lambda_{qs} - V_{ds} \quad (1)$$

$$\frac{1}{\omega_s}\frac{d}{dt}\lambda_{qs} = -R_s I_{qs} - \lambda_{ds} - V_{qs} \quad (2)$$

$$\frac{1}{\omega_s}\frac{d}{dt}\lambda_{dr1} = -R_{r1} I_{dr1} + s\lambda_{qr1} \quad (3)$$

$$\frac{1}{\omega_s}\frac{d}{dt}\lambda_{qr1} = -R_{r1} I_{qr1} - s\lambda_{dr1} \quad (4)$$

$$\frac{1}{\omega_s}\frac{d}{dt}\lambda_{dr2} = -R_{r2} I_{dr2} + s\lambda_{qr2} \quad (5)$$

$$\frac{1}{\omega_s}\frac{d}{dt}\lambda_{qr2} = -R_{r2} I_{qr2} - s\lambda_{dr2} \quad (6)$$

where, the flux linkage equations are:

$$\lambda_{ds} = X_s I_{ds} + X_m I_{dr1} + X_m I_{dr2} \quad (7)$$

$$\lambda_{qs} = X_s I_{qs} + X_m I_{qr1} + X_m I_{qr2} \quad (8)$$

$$\lambda_{dr1} = X_m I_{ds} + X_{r1} I_{dr1} + X_{12} I_{dr2} \quad (9)$$

$$\lambda_{qr1} = X_m I_{qs} + X_{r1} I_{qr1} + X_{12} I_{qr2} \quad (10)$$

$$\lambda_{dr2} = X_m I_{ds} + X_{12} I_{dr1} + X_{r2} I_{dr2} \quad (11)$$

$$\lambda_{qr2} = X_m I_{qs} + X_{12} I_{qr1} + X_{r2} I_{qr2} \quad (12)$$

In which

$$X_{12} = X_m + X_{rm} \quad (13)$$

$$X_s = X_{s\sigma} + X_m \quad (14)$$

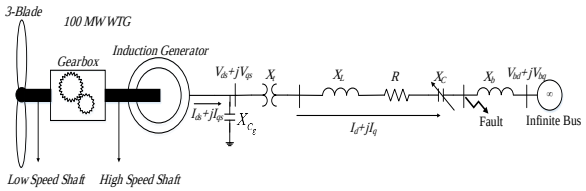

Figure 1. The studied system

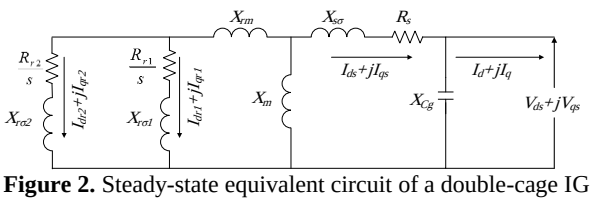

Figure 2. Steady-state equivalent circuit of a double-cage IG

$$X_{r1} = X_{r1\sigma} + X_{12} \tag{15}$$

$$X_{r2} = X_{r2\sigma} + X_{12} \tag{16}$$

The generator electromagnetic torque (T_G) is expressed as follows:

$$T_G = X_m \left[I_{ds}(I_{qr1} + I_{qr2}) - I_{qs}(I_{dr1} + I_{dr2}) \right] \tag{17}$$

2. 2. Wind Turbine Generator Model In each model, the speed of each mass and the angle between two adjacent ones are considered as state variables. Therefore, in 6-mass, 4-mass, 3-mass I, 3-mass II, 2-mass and 1-mass models, respectively, 11, 7, 5, 5, 3 and 2 differential equations are considered.

In this section, different multi mass models are considered to model the wind-turbine generator. These models are presented as 6-mass, 4-mass, 3-mass I, 3-mass II, 2-mass and 1-mass. The detailed equations of these models can be found in [8-9] and their schematic diagrams are shown in Figure 3. The 6-mass model consists of three blade inertias (H_{B1}, H_{B2} and H_{B3}), hub inertia (H_H), gearbox inertia (H_{GB}), and generator inertia (H_G). In the 4-mass model, the three-blade turbine is considered as one mass and the turbine torque is equal to the summation of the blades torque. In the 4-mass model, by adding some masses together the two model of 3-mass can be provided. The 3-mass I model can be obtained by adding the blade and hub inertias together (H_{BH}); while the 3-mass II model can be acquired by adding the gearbox and generator inertias (H_{GBG}). The 2-mass model is developed from 3-mass I model by adding the gearbox and generator inertias together (H_{GBG}). Finally, in order to make a comparison with a rigid model, 1-mass model is considered as shown in Figure 3.

2. 3. Network Model The differential equations of the transmission line are given by the following equations:

$$\frac{1}{\omega_s}\frac{d}{dt}V_{ds} = X_{C_g} I_{ds} - X_{C_g} I_d + V_{qs} \tag{18}$$

$$\frac{1}{\omega_s}\frac{d}{dt}V_{qs} = X_{C_g} I_{qs} - X_{C_g} I_q - V_{ds} \tag{19}$$

$$\frac{1}{\omega_s}\frac{d}{dt}I_d = \frac{1}{X}V_{ds} - \frac{R}{X}I_d + I_q - \frac{1}{X}V_{cd} - \frac{1}{X}V_{bd} \tag{20}$$

$$\frac{1}{\omega_s}\frac{d}{dt}I_q = \frac{1}{X}V_{qs} - \frac{R}{X}I_q - I_d - \frac{1}{X}V_{cq} - \frac{1}{X}V_{bq} \tag{21}$$

$$\frac{1}{\omega_s}\frac{d}{dt}V_{cd} = X_C I_d + V_{cq} \tag{22}$$

$$\frac{1}{\omega_s}\frac{d}{dt}V_{cq} = X_C I_q - V_{cd} \tag{23}$$

In addition, X is defined as:

$$X = X_L + X_t + X_b \tag{24}$$

In a compensated transmission line, series compensation parameter (K) is defined as:

$$K = \frac{X_C}{(X_L + X_t)} \times 100 \tag{25}$$

3. SMALL SIGNAL ANALYSIS

The wind farm in the study system is consisting of 50 numbers of double-cage IGs. The rated capacity of each generator is 2MW at unity power factor. Potential for SSR interactions is investigated by considering an equivalent model of wind-turbine generators and increasing the series compensation level (K) from 10% to 90%. For the SSR analysis, sub-synchronous and torsional modes are of interest.

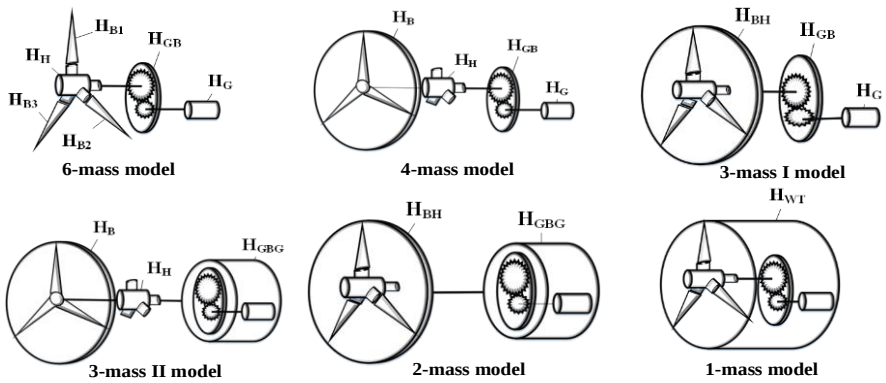

Figure 3. Schematic diagram of wind turbine-generator shaft models.

Therefore, the effects of the wind turbine-generator shaft models and series compensation level on the damping of these modes are studied. At first, for different models of wind-turbine, by linear modal analysis, the eigenvalues of the test system are obtained at the operating point (100 MW wind farm and 50% series compensation level), and the results are shown in Table 1.

3. 1. Sub-synchronous Mode According to Table 1, the sub-synchronous mode is found to be less stable, but it is not affected by wind turbine-generator shaft model. This subject needs to be further investigated. Therefore, by using linear modal analysis, the participation matrix is obtained and the participation of system components on the sub-synchronous mode is presented in Figure 4. As is observed, the mechanical parameters have little effect on this mode. Hence, the different wind turbine-generator shaft models have negligible effect on the sub-synchronous mode.

For six considered models of wind-turbine generator shafts, the eigenvalue variations of the sub-synchronous mode are obtained for different series compensation levels, and the results are shown in Figure 5. As seen, as the series compensation level increases, the damping of the sub-synchronous mode decreases. At a certain critical compensation level (55.48%), this mode becomes unstable and indicates the onset of IG self-excitation.

3. 2. Torsional Modes Figure 6 shows the displacement of the torsional modes in the 6-mass wind turbine-generator shaft model for different levels of series compensation.

TABLE 1. Eigenvalues of the test system at the operating point.

Modes Type	Different Wind Turbine-Generator Shaft Models					
	1-mass model	2-mass model	3-mass I model	3-mass II model	4-mass model	6-mass model
Network mode-1	-7.53 ± j1978.67	-7.53 ±j1978.70	-7.53±j1978.71	-7.53±j1978.70	-7.53±j1978.71	-7.53±j1978.71
Network mode-2	-8.97 ± j1224.63	-8.97±j1224.69	-8.97±j1224.73	-8.97±j1224.69	-8.97±j1224.73	-8.97±j1224.73
Super-synchronous mode	-6.98 ± j516.05	-6.98 ± j516.13	-6.99 ± j516.19	-6.98 ± j516.13	-6.99 ± j516.19	-6.99 ± j516.19
Sub-synchronous mode	-0.431 ± j237.87	-0.411±j237.50	-0.394±j237.21	-0.411±j237.50	-0.394±j237.21	-0.394±j237.21
Rotor mode	-64.15 ± j3.27	-63.38 ± j3.12	-63.14 ± j3.01	-63.39 ± j3.12	-63.14 ± j3.01	-63.14 ± j3.01
Electromechanical mode	-5.97 ± j12.82	-5.91 ± j30.40	-5.03 ± j30.02	-5.81 ± j29.25	-4.80 ± j28.14	-4.80 ± j28.14
Flux mode	-8.788	-9.052	-9.060	-9.070	-9.081	-9.081
Torsional mode 1	-	-0.756 ± j5.390	-0.767 ± j5.374	-0.579 ± j4.755	-0.538 ± j4.557	-0.538 ± j4.557
Torsional mode 2	-	-	-	-1.246±j42.080	-1.434 ± j41.89	-1.434 ± j41.89
Torsional mode 3	-	-	-2.299 ± j67.99	-	-2.286 ± j68.26	-2.286 ± j68.26
Torsional mode 4	-	-	-	-	-	-0.046 ± j8.353
Torsional mode 5	-	-	-	-	-	-0.046 ± j8.353

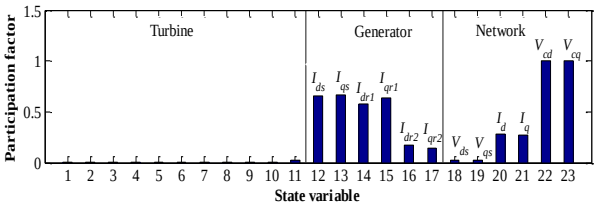

Figure 4. Participation level of system components on the sub-synchronous mode.

According to Figure 6, the damping ratio of the first, second and third torsional modes decreases steadily with the increase in the level of series compensation.

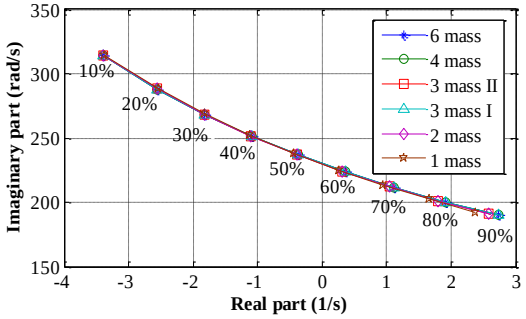

Figure 5. Displacement of sub-synchronous mode in different wind turbine-generator shaft models, when the series compensation level is increased.

However, none of the torsional modes are unstable. In addition, the damping ratio of fourth and fifth torsional modes is not affected by series compensation. Since the damping of some torsional modes are affected by the series compensation, to SSR analysis of wind farms based double-cage IGs, considering an appropriate model of the wind turbine-generator shaft is very important.

The first, second and third torsional modes that affected by series compensation are detected by 4-mass and 6-mass shaft models. The only difference between these two models is that in the 6-mass shaft model, the blades are modeled individually.

The participation of system components on the torsional modes is shown in Figure 7.

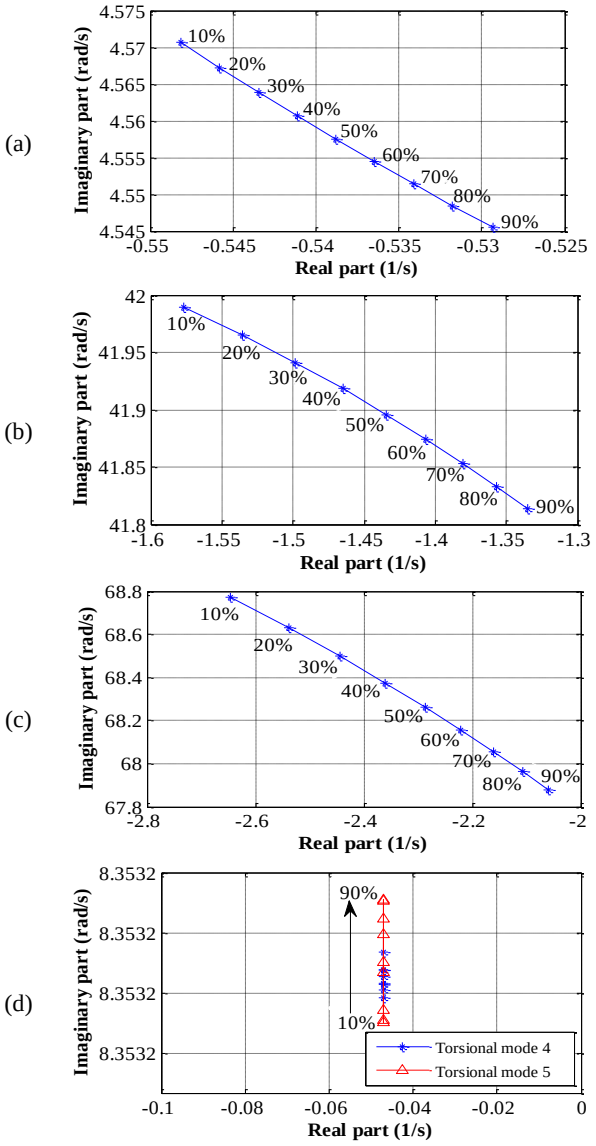

Figure 6. Displacement of torsional modes for different compensation levels: (a) Torsional mode 1, (b) Torsional mode 2, (c) Torsional mode 3, (d) Torsional modes 4 & 5

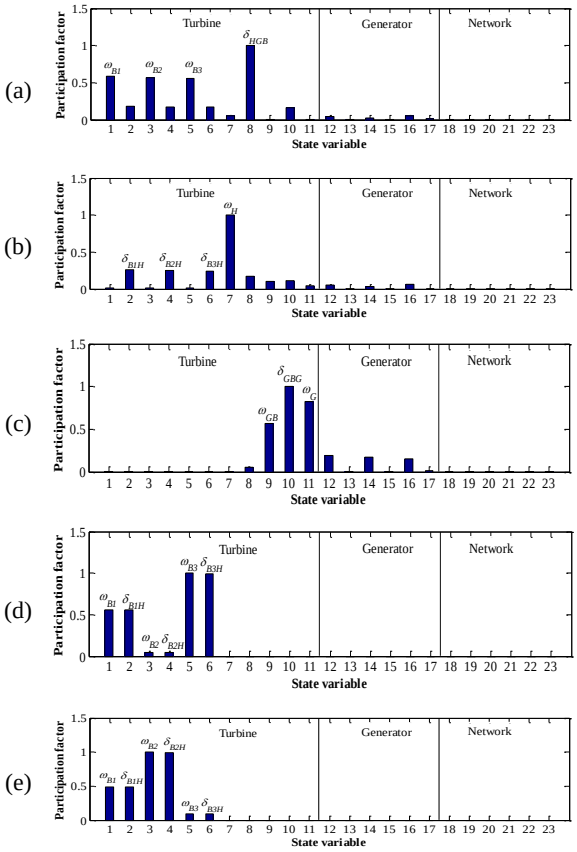

Figure 7. Participation level of system components on the torsional modes: (a) Torsional mode 1, (b) Torsional mode 2, (c) Torsional mode 3, (d) Torsional mode 4, (e) Torsional mode 5

As seen, the blades have most participation on the torsional modes 4 and 5. Since these torsional modes are not affected by series compensation (see Figure 6), the 4-mass model can be considered as an appropriate model for wind-turbine generator in the SSR analysis of double-cage IG based wind farm.

4. SIMULATION

To validate the obtained results from small signal analysis a detailed electromagnetic transient simulation is done with the PSCAD/EMTDC software. Fault studies are conducted for a LLLG fault for 6 cycles (100ms) at the end of the transmission line. In addition, the 6-mass shaft model is considered for wind turbine-generator shaft.

4. 1. Steady-state Condition To validate the system model used for small signal analysis, the steady-state solution of the 6-mass shaft model is compared with the results obtained from the electromagnetic transient simulation. By considering different

aerodynamic torques, the variables active output power (P_g), reactive output power (Q_g), terminal voltage of the wind farm (V_s), and the speed of the generator (ω_g) are calculated for 50% series compensation, and the results are shown in Table 2.

As seen, in all cases, both the results of the system used for small signal analysis and PSCAD are matched very closely, which validates the small signal model in the steady-state condition.

4. 2. Transient Condition In Section 3, it is shown that by increasing the series compensation level, the damping of some system modes is affected. To validate the obtained analytical results, the test system is simulated at 50% and 60% series compensation levels and some results are shown in Figure 8 and Figure 9. The important eigenvalues of the test system for these series compensation levels obtained by small signal analysis are provided in Table 3.

Since the 50% series compensation, is a stable operating condition (as seen from Table 3, all eigenvalues have negative real part in 50% compensation level), Figure 8 shows that the system oscillations are decayed in this compensation level. However, with 60% series compensation because of instability of sub-synchronous mode (as seen from Table 3, the sub-synchronous mode has positive real part in 60% compensation level), the electromagnetic torque and the torsional torque between gearbox and generator grow gradually and become unstable (Figure 9).

TABLE 2. Steady-state results of the system model used for small signal analysis and transient simulation.

System Variables	aerodynamic torque=1pu		aerodynamic torque=0.5pu	
	system model used for small signal analysis	PSCAD	system model used for small signal analysis	PSCAD
P_g (pu)	0.994	0.993	0.498	0.494
Q_g (pu)	-0.510	-0.510	-0.323	-0.324
V_s (pu)	1.022	1.021	1.029	1.028
ω_g (pu)	1.008	1.007	1.003	1.003

TABLE 3. Important eigenvalues of the test system at 50% and 60% series compensation levels.

Modes	50% Series compensation	60% Series compensation
Sub-synchronous mode	-0.394 ± j237.21	0.321 ± j224.17
Torsional mode 1	-0.538 ± j4.55	-0.536 ± j4.55
Torsional mode 2	-1.434 ± j41.89	-1.406 ± j41.87
Torsional mode 3	-2.286 ± j68.26	-2.220 ± j68.15

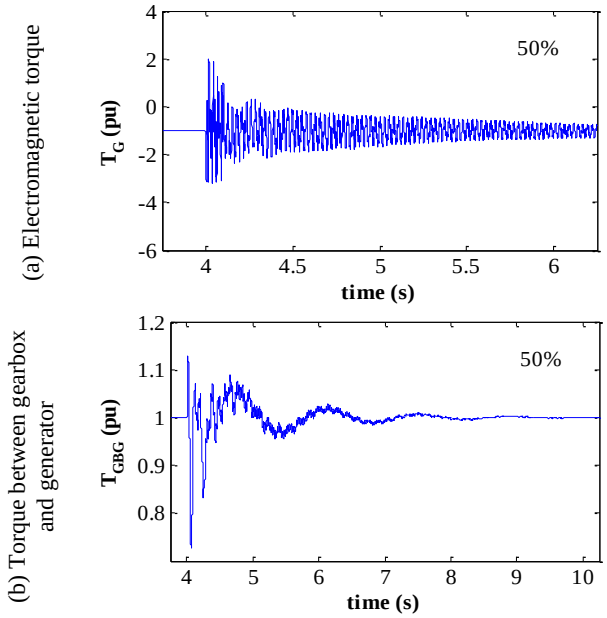

Figure 8. Transient SSR in the test system for 50% series compensation

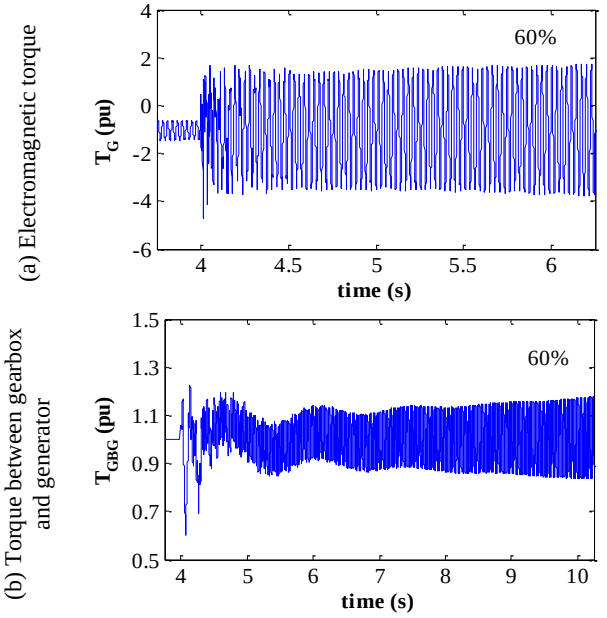

Figure 9. Transient SSR in the test system for 60% series compensation

In addition, although with 60% series compensation, other torsional torques are stable but because of decreasing of the torsional modes damping, the amplitude of torsional oscillations is increased.

The FFT of electromagnetic and shaft torques at 50% and 60% series compensation levels, respectively, are shown in Figure 10 and Figure 11. Comparing the FFT results with the analytical results in Table 3, indicates that in all cases, the frequencies obtained from small signal analysis are very close to frequencies detected by FFT.

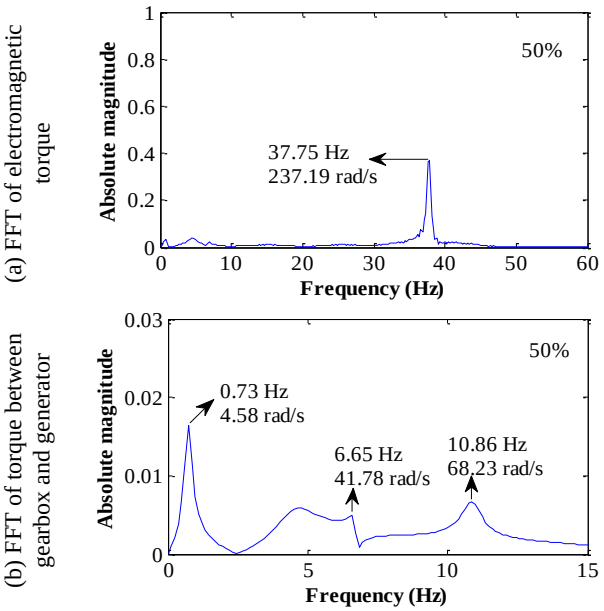

Figure 10. FFT analysis of transient SSR in the test system for 50% series compensation

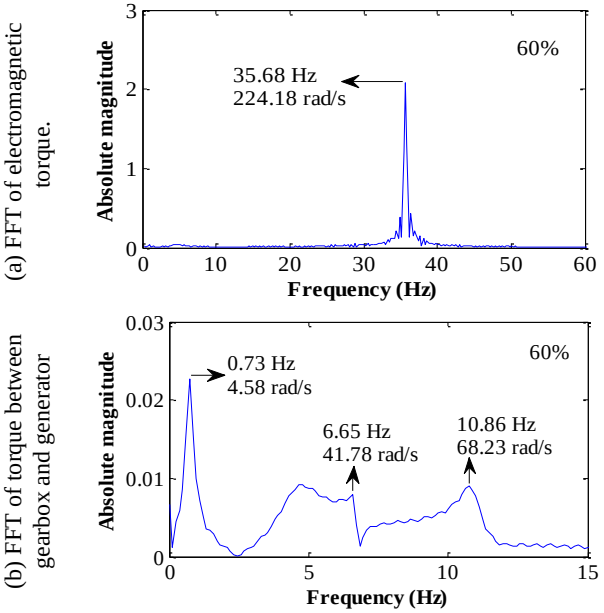

Figure 11. FFT analysis of transient SSR in the test system for 60% series compensation

For instance, at 60% series compensation in the FFT of electromagnetic torque (Figure 11(a)) the detected frequency, 224.18 rad/s, matches with the frequency 224.17 rad/s which is obtained from small signal analysis (see Table 3). In addition, as the FFT of electromagnetic torque at 60% series compensation reveals the excitation of the frequency 224.18 rad/s, instability of this mode is shown by the small signal analysis (see Table 3).

5. CONCLUSION

This paper presents a detailed analysis of the effect of different wind turbine-generator shaft models of double-cage IG on the potential of SSR in the wind farm connected to the series compensated transmission line. The sub-synchronous mode is found to be the most sensitive among all modes and tends to become less stable (or unstable) with an increase in series compensation. The results show that different models of the wind-turbine generator have little effect on the sub-synchronous mode. In addition, the damping ratio of some torsional modes decreases with an increase in the level of series compensation, but none of the torsional modes are unstable. The torsional modes affected by series compensation, can be detected by 6-mass and 4-mass shaft models. Therefore, to SSR analysis of double-cage IG based wind farm, the 4-mass model is proposed as an appropriate model for wind-turbine generator shaft.

6. REFERENCES

1. Hau, E., Wind turbines (fundamentals, technologies, application, economics). 2006, Berlin, Germany.
2. Anaya-Lara, O., Ekanayake, J. and Huges, C., "Wind energy generation modeling and control", in John Wiley and Sons, Chichester, UK., (2009).
3. Savio, M. and Murugesan, S., "Space vector control scheme of three level zsi applied to wind energy systems", ***International Journal of Engineering-Transactions C: Aspects***, Vol. 25, No. 4, (2012), 275-282.
4. Akhmatov, V., Induction generators for wind power, Multi-Science Pub., (2005).
5. Kundur, P., Balu, N.J. and Lauby, M.G., "Power system stability and control, McGraw-hill New York, Vol. 7, (1994).
6. Padiyar, K., Analysis of subsynchronous resonance in power systems, Springer Science & Business Media, (2012).
7. Widyan, M.S., "On the effect of avr gain on bifurcations of subsynchronous resonance in power systems", ***International Journal of Electrical Power & Energy Systems***, Vol. 32, No. 6, (2010), 656-663.
8. Papathanassiou, S.A. and Papadopoulos, M.P., "Mechanical stresses in fixed-speed wind turbines due to network disturbances", ***IEEE Transactions on Energy Conversion***, Vol. 16, No. 4, (2001), 361-367.
9. Muyeen, S., Ali, M.H., Takahashi, R., Murata, T., Tamura, J., Tomaki, Y., Sakahara, A. and Sasano, E., "Transient stability analysis of wind generator system with the consideration of multi-mass shaft model", in 2005 International Conference on Power Electronics and Drives Systems, IEEE. Vol. 1, (2006), 511-516.
10. Li, H. and Chen, Z., "Transient stability analysis of wind turbines with induction generators considering blades and shaft flexibility", in Industrial Electronics Society, 2007. IECON 2007. 33rd Annual Conference of the IEEE, (2007), 1604-1609.
11. Muyeen, S., Ali, M.H., Takahashi, R., Murata, T., Tamura, J., Tomaki, Y., Sakahara, A. and Sasano, E., "Comparative study on transient stability analysis of wind turbine generator system

using different drive train models", ***IET Renewable Power Generation***, Vol. 1, No. 2, (2007), 131-141.

12. Xu, Z. and Pan, Z., "Influence of different flexible drive train models on the transient responses of dfig wind turbine", in Electrical Machines and Systems (ICEMS), 2011 International Conference on, IEEE., (2011), 1-6.
13. Han, X., Wang, P., Wang, P. and Qin, W., "Transient stability studies of doubly-fed induction generator using different drive train models", in Power and Energy Society General Meeting, IEEE., (2011), 1-6.
14. Wamkeue, R., Chrourou, Y., Song, J. and Nyobe-Yome, J.M., "State modeling based prediction of torsional resonances for horizontal-axis drive train wind turbine", in Renewable Power Generation (RPG 2011), IET, (2011), 1-4.
15. Ostadi, A., Yazdani, A. and Varma, R.K., "Modeling and stability analysis of a dfig-based wind-power generator interfaced with a series-compensated line", ***IEEE Transactions on Power Delivery***, Vol. 24, No. 3, (2009), 1504-1514.
16. Fan, L., Zhu, C., Miao, Z. and Hu, M., "Modal analysis of a dfig-based wind farm interfaced with a series compensated network", ***IEEE Transactions on Energy Conversion***, Vol. 26, No. 4, (2011), 1010-1020.
17. Moharana, A. and Varma, R.K., "Subsynchronous resonance in single-cage self-excited-induction-generator-based wind farm connected to series-compensated lines", ***IET generation, transmission & distribution***, Vol. 5, No. 12, (2011), 1221-1232.
18. Mohammadpour, H.A., Ghaderi, A. and Santi, E., "Analysis of sub-synchronous resonance in doubly-fed induction generator-based wind farms interfaced with gate–controlled series capacitor", ***IET Generation, Transmission & Distribution***, Vol. 8, No. 12, (2014), 1998-2011.
19. Leon, A.E., Mauricio, J.M. and Solsona, J.A., "Subsynchronous resonance mitigation using variablespeed wind energy conversion systems", ***IET Generation, Transmission & Distribution***, Vol. 7, No. 5, (2013), 511-525.
20. Varma, R.K. and Moharana, A., "Ssr in double-cage induction generator-based wind farm connected to series-compensated transmission line", ***IEEE Transactions on Power Systems***, Vol. 28, No. 3, (2013), 2573-2583.
21. Mohammadpour, H.A. and Santi, E., "Sub-synchronous resonance analysis in dfig-based wind farms: Definitions and problem identification—part I", in Energy Conversion Congress and Exposition (ECCE), IEEE., (2014), 812-819.
22. Moharana, A., Varma, R.K. and Seethapathy, R., "Ssr alleviation by statcom in induction-generator-based wind farm connected to series compensated line", ***IEEE Transactions on Sustainable Energy***, Vol. 5, No. 3, (2014), 947-957.
23. Xi, X., Geng, H. and Yang, G., "Enhanced model of the doubly fed induction generator-based wind farm for small-signal stability studies of weak power system", ***IET Renewable Power Generation***, Vol. 8, No. 7, (2014), 765-774.
24. Mancilla-David, F., Dominguez-Garcia, J.L., De Prada, M., Gomis-Bellmunt, O., Singh, M. and Muljadi, E., "Modeling and control of type-2 wind turbines for sub-synchronous resonance damping", ***Energy Conversion and Management***, Vol. 97, (2015), 315-322.
25. Besanjideh, M. and Mahani, M.F., "Nonlinear and non-stationary vibration analysis for mechanical fault detection by using emd-fft method", ***International Journal of Engineering-Transactions C: Aspects***, Vol. 25, No. 4, (2012), 363-372.

7. APPENDIX

TABLE A. 1. Double-cage induction generator data.

Parameter	Value	Parameter	Value
P	2 MW	R_{r2} (pu)	0.019239
V	690 V	$X_{r\sigma 1}$ (pu)	0
f	60 Hz	$X_{r\sigma 2}$ (pu)	0.21172
R_S (pu)	0.00506	X_{rm} (pu)	0.072175
$X_{s\sigma}$ (pu)	0.13176	X_m (pu)	3.8892
R_{r1} (pu)	0.01199	Pole-pair number	3

TABLE A. 2. Transmission line data.

Parameter	Value	Parameter	Value
System Base	892.4 MVA	R	0.02 pu
Base Voltage	500 kV	X_b	0.06 pu
X_t	0.14 pu	X_c	(10% - 90%)* (X_t + X_L)
X_L	0.50 pu		

TABLE A. 3. Wind-turbine 2 MW data.

Parameter	Value	Parameter	Value
Rotor diameter	80 m	Turbine rotor speed	13.5 rpm
Number of blades	3	Gearbox ratio	88.8
Machine rated mechanical speed	1200 rpm	Air density	1.225 kg/m^3

Effect of Different Turbine-generator Shaft Models on the Sub-synchronous Resonance Phenomenon in the Double Cage Induction Generator Based Wind Farm

M. K. Salehi, R. Zeinali Davarani

Faculty of Electrical and Computer Engineering, Graduate University of Advanced Technology, Kerman, Iran

P A P E R I N F O

Paper history:
Received 07 February 2016
Received in revised form 14 July 2016
Accepted 14 July 2016

Keywords:
Double Cage Induction Generator
Turbine-Generator Shaft Model
Wind Farm
Torsional Modes
Sub-Synchronous Resonance

چکیده

این مقاله بر روی مدل‌های شفت توربین–ژنراتور یک مزرعه بادی مبتنی بر ژنراتور القایی دو قفسه و اثر آن بر روی پدیده تشدید زیر سنکرون تمرکز می‌کند. برای این منظور شش مدل شفت مختلف به صورت شش جرمه، چهار جرمه، سه جرمه نوع اول، سه جرمه نوع دوم، دو جرمه و تک جرمه برای توربین بادی مبتنی بر ژنراتور القایی دو قفسه لحاظ شده است. با استفاده از روش تحلیل مُدال خطی، اثر مدل چند جرمه مختلف از توربین بادی با ژنراتور القایی دو قفسه بر پدیده تشدید زیر سنکرون مطالعه شده است. نتایج بدست آمده توسط تحلیل مقدار ویژه نشان می‌دهد که مدل توربین بادی با ژنراتور القایی دو قفسه یک اثر مهم بر روی تشخیص پدیده تشدید زیر سنکرون دارد. نتایج تحلیلی توسط شبیه‌سازی گذرای الکترومغناطیسی با استفاده از نرم افزار PSCAD/EMTDC تایید شده است.

***doi**: 10.5829/idosi.ije.2016.29.08b.10*